Journal of Building Engineering 84 (2024) 108517

Contents lists available at ScienceDirect

Journal of Building Engineering

journal homepage: www.elsevier.com/locate/jobe

# Impact of $SiO_2$, $TiO_2$ and ZnO nanoparticles incorporation on the thermo-optical properties of dark-coloured façade coatings

Rita Carvalho Veloso [a,b], Joana Maia [a,*], Rodrigo Praça [a], Andrea Souza [a], João Ventura [b], Nuno M.M. Ramos [a], Helena Corvacho [a]

[a] CONSTRUCT-LFC, Departamento de Engenharia Civil, Faculdade de Engenharia, Universidade do Porto, Rua Dr. Roberto Frias, 4200-465, Porto, Portugal

[b] IFIMUP, Departamento de Física e Astronomia, Faculdade de Ciências, Universidade do Porto, Rua do Campo Alegre s/n, 4169–007, Porto, Portugal

ARTICLE INFO

*Keywords:*
Thermo-optical properties
Colour properties
Spectrophotometer
Nanoparticles
Façade

ABSTRACT

In pursuing energy-efficient construction and reduced environmental impact, this study explores the integration of $TiO_2$, $SiO_2$, and ZnO nanoparticles into coatings for thermal-enhanced façade systems. Buildings account for a substantial portion of energy consumption, with façades playing a pivotal role. The impact of nanoparticle type, size, and material combination on thermo-optical performance was investigated through systematic analysis.

Our findings reveal significant improvements in near-infrared (NIR) reflectance, a crucial factor in minimising heat absorption. Notably, $TiO_2$ nanoparticles demonstrate a 50 % enhancement in NIR reflectance with a colour difference (ΔE) of 3.4, followed by ZnO (28 %, ΔE 3.2) and $SiO_2$ (22 %, ΔE 4.61). Application-specific variations highlight the improved behaviour of $TiO_2$ in coatings for ETICS (Exterior Thermal Insulation Composite Systems), $SiO_2$ in acrylic paints, and ZnO in dye formulations.

These results allow architects and builders to incorporate dark colours into façade aesthetics while maintaining thermo-optical efficiency and durability. As the demand for sustainable building practices grows, our work contributes to the evolving landscape of energy-efficient construction materials and design strategies. Investigating the long-term durability of these nanoparticle-enhanced coatings remains an important future research avenue.

## 1. Introduction and background

Energy consumption has become a significant concern in economic development and an important issue to solve in the decarbonisation pathway. According to the European Commission [1], 40 % of the energy consumption is attributed to buildings, which are highly related to the operation stage for indoor space comfort, heating or cooling needs, as stated by several authors [2–7]. This fact dramatically impacts greenhouse gas emissions, of which buildings are responsible for 36 % [1]. Furthermore, the durability requirement applied to construction materials and components is crucial to ensure sustainable construction, reducing the need for new resources and reducing waste.

Unavoidably, when exposed to solar radiation, buildings absorb a large portion of the radiation reaching their exterior surface [8]. Building envelopes may reach very high temperatures depending on their surface properties, such as reflectance and emissivity.

* Corresponding author.
*E-mail address:* joanamaia@fe.up.pt (J. Maia).

https://doi.org/10.1016/j.jobe.2024.108517
Received 8 September 2023; Received in revised form 3 January 2024; Accepted 11 January 2024
Available online 20 January 2024

Studies focusing on the search for mechanisms that increase reflectance in the near-infrared region (NIR) are being conducted with increasing intensity [9–11].

Reducing the building envelope exterior surface temperature may reduce indoor cooling energy needs, especially in old buildings with a low level of thermal insulation, thus promoting thermal comfort for building users [12]. However, as stated in Cánovas-Saura et al. [13], including additional thermal insulation in a realistic building design makes possible savings due to the use of reflective finishing negligible, especially for colder climates. Thus, in new buildings with a higher level of thermal insulation, the main concern is not related to indoor thermal comfort or energy consumption but to the fact that the outer layers of the façade, when exposed to solar radiation, are particularly prone to thermal stress, which means higher surface temperatures and greater temperature variations. This may have a significant impact on their durability.

The colour of building façades plays an essential role due to its influence on the temperature reached by the coating layers when exposed to solar radiation. The temperature is usually higher on a dark tone façade than on a light tone façade [14]. Consequently, the dark tone façades are more prone to degradation due to high-temperature variations. Cánovas-Saura et al. [13] studied the possibilities of obtaining efficient thermal control in buildings by means of coloured envelopes while maintaining broad aesthetic options. Their study focused on using coloured bilayers, where the inner layer presents strong solar absorbance or reflectance properties while the outer layer provides visible colouration. The use of bilayers broadened the envelope colour range while achieving energy savings, particularly in hot climates and for a low level of thermal insulation.

In countries where summer overheating is a concern, painting the façades with light or white colour is widespread and an old practice. White effectively reflects solar radiation in the visible region as well as in the NIR region, as well as absorbing a very low amount of the incident total solar radiation [15]. A smooth, opaque and white surface can reach 85 % of solar reflectance [16]. However, such a high reflectance value corresponds to a clean and white surface. Over time, the reflectance of exposed façades tends to decrease due to dust deposition and the natural ageing of the paints. Cheng et al. [17] and Wu et al. [18] observed that the solar reflectance decreases by 20–50 % due to the deposition of dust and soot. Dust and soot deposition mainly affect reflectance in the visible range between 400 and 700 nm. It results from physical weathering due primarily to black carbon and automobile exhaust dust deposition [19].

Besides, sometimes architects show a preference for dark colours for façade coating layers. Some of the reasons influencing this choice are related to the aesthetics and the ease with which dark-tone façades disguise dirt and pollution caused by atmospheric agents [15,16]. Furthermore, a façade with light colours can increase the risk of external surface condensation in colder periods, accelerating degradation due to biological growth [20,21].

To our knowledge, only a few studies focused on dark NIR-reflective pigments. Suwan et al. [22] described a Co-doped $ZnFe_2O_4$ black pigment synthesis with a 48–50 % NIR reflectance. Wang et al. [23] prepared a $MnTiO_3$ powder with a good solar use performance. However, these pigments require complex syntheses with difficult implementation in the industry, high energy demand (due to calcination processes) and solvents that are not considered environmentally friendly.

Cozza et al. [24] presented a study on the possible formulation of exterior building paints as smart coatings with high IR-reflectance to decrease energy use for cooling buildings. This strategy aimed to broaden the range of colours of the urban aesthetic to the dark ones, overtaking the current white-cool solutions. The study focused on black pigments, considering their use for producing both black paints and different shades of grey colours. Increments of 30 % were found for total solar reflectance.

Given the choice of dark tones, incorporating nanomaterials in the façade finishing layer is one of the possible solutions to avoid excessive solar absorptance. Thus, the nanomaterials chosen are generally metallic oxides, given their great capacity to selectively reflect solar radiation in the visible and near-infrared region [25]. Organic materials can have the same capacity, although these materials tend to suffer photodegradation with UV exposure [25]. Titanium dioxide ($TiO_2$) is a metal oxide that effectively contributes to solar reflectance [26]. Besides $TiO_2$, another promising nanomaterial is zinc oxide (ZnO). Due to its stability in harsh chemical and mechanical conditions and low toxicity, it is widely used in decorative paints. However, it cannot scatter light like $TiO_2$ [27].

The optical properties of nanomaterials, such as emissivity and reflectance, are strongly connected with particle size. As the particle size decreases, the density of the sample changes and consequently, the reflectance is affected [28,29]. Besides providing an effect on the thermal performance of façades, nanomaterials may help to improve the physical properties of materials such as mortars, enhance the durability of composite materials, allow for materials weight reduction, as well as provide antimicrobial, anti-corrosive and self-cleaning properties [25,30,31].

To test the application of titanium dioxide ($TiO_2$) on travertine stones, research was carried out on their durability. The results showed that using nanoparticles of both $TiO_2$ polymorphs (rutile and anatase) dispersedly in resin significantly increased the durability of the surfaces of the stones during the ageing tests. No colour change in the sample surfaces is another advantage of the resin-$TiO_2$ nanoparticle hybrid coating. The best performance was obtained with anatase $TiO_2$ nanoparticles since they are colourless powder [32].

An article on photocatalytic $TiO_2$-based thin layers to be applied on mortars in façades, which concerns coating efficiency, confirms the beneficial photocatalytic activity of the coating and identifies the needs for further research. The latter would be mainly on specific evaluations that may be needed for each coating composition and testing condition to understand their performance. The type of contamination agents, $TiO_2$ dispersion and characteristics, dopants, nanocomposites and type of substrate are among the principal agents influencing the results [33].

Lu et al. [34] also used nanoparticles to develop a colourful superhydrophobic coating of silicon dioxide nanoparticles ($SiO_2$), quartz sands, silicone sealant, and latex paint. The produced coating meets both durability and aesthetic requirements and shows mechanical stability, anti-corrosion characteristics and high UV resistance [34].

In the scope of a broader research project, Circular2B, the present study investigates the influence of three reflective nanomaterials ($TiO_2$, $SiO_2$ and ZnO) on the thermo-optical properties of façade coatings, aiming to assess the suitability of newly formulated coatings

with nanoparticles incorporation. As such, the main objective focuses on enhancing the reflectance of dark surfaces in the NIR region without changing their colour. Those coatings are applied to an External Thermal Insulation Composite System (ETICS), the most commonly used thermal insulation system in Portugal, particularly in renovation actions, and a cladding panel. This panel is made of an alkali-activated (AA) mortar mainly composed of industrial and construction and demolition wastes (CDW), which are being studied and optimised to respond to the growing need to apply circular construction principles.

## 2. Materials and methods

This study aimed to analyse the effect of the selected nanoparticles' incorporation in two distinct stages, as shown in Fig. 1. In the first phase, the nanoparticles were dispersed directly in the matrices (black colourant and black water-based acrylic paint) in different concentrations (1, 3, 5, 8, 12, 16 and 20 % w/w) to investigate the impact on black colourants commonly used to formulate finishing coatings. In the second stage, the adequate percentage of nanoparticles found in the first stage was selected to be incorporated in the finishing coatings of two distinct façade systems (ETICS and AA cladding panel). The percentage of nanoparticles was defined to maximise reflectance in the near-infrared and minimise the colour difference of the surface of façade systems.

### 2.1. Materials and sample preparation

Three types of nanoparticles with distinct dimensions were selected and purchased from an external supplier, as described in Table 1. All nanopowders used in this study were ≥99.9 % trace metals basis and were employed as obtained without further purification.

For the first stage, all the modified samples were mixed at room temperature, until a homogeneous mixture, and then applied on 35 × 35 × 3 $mm^3$ acrylic substrates with a spatula. The standard matrices are a commercial black iron oxide-base dispersion colourant (PBk11 index) for the ETICS finishing coating and an acrylic water-based paint (PBk7 index) commonly used on façade systems for coating the cladding panel. The properties of such black coating are described in Table 2.

After the production and subsequent analysis of the reflectance and colour, despite all samples increased the total and NIR reflectance when compared to the conventional colourant and to the acrylic paint, it was found that the adequate percentage to modify the commercial finishing coatings was 8 % (% w/w). As such, ETICS and cladding samples were produced with nanoparticles incorporated in their finishing coatings, as shown in Table 3.

Four certified and commercial ETICS samples were produced and tested based on the EAD 040083-00-0404 [35]. The ETICS, according to the information provided by the manufacturers, have EPS (expanded polystyrene, 20 kg/$m^3$) as thermal insulation with a thickness of 60 mm and a base coat composed of cement, synthetic resins and mineral additives, with density between 1700 and 1800 kg/$m^3$, applied with 1–2 mm. The base coat layer was reinforced by a glass fibre mesh. The finishing coating is an acrylic-based material with organic additives, incorporating 6 % of a black colourant mixed or not with nanoparticles. The manufacturers frequently use this percentage of the black colourant to provide the black tone to the finishing coatings.

Four cladding samples were produced from industrial, construction, and demolition wastes. Mainly, they are constituted of fly ash (90 % w/w), polyurethane (% 5 w/w), timber (% 5 w/w) and aluminium powder (<0.1 % w/w). The mixtures were alkali-activated

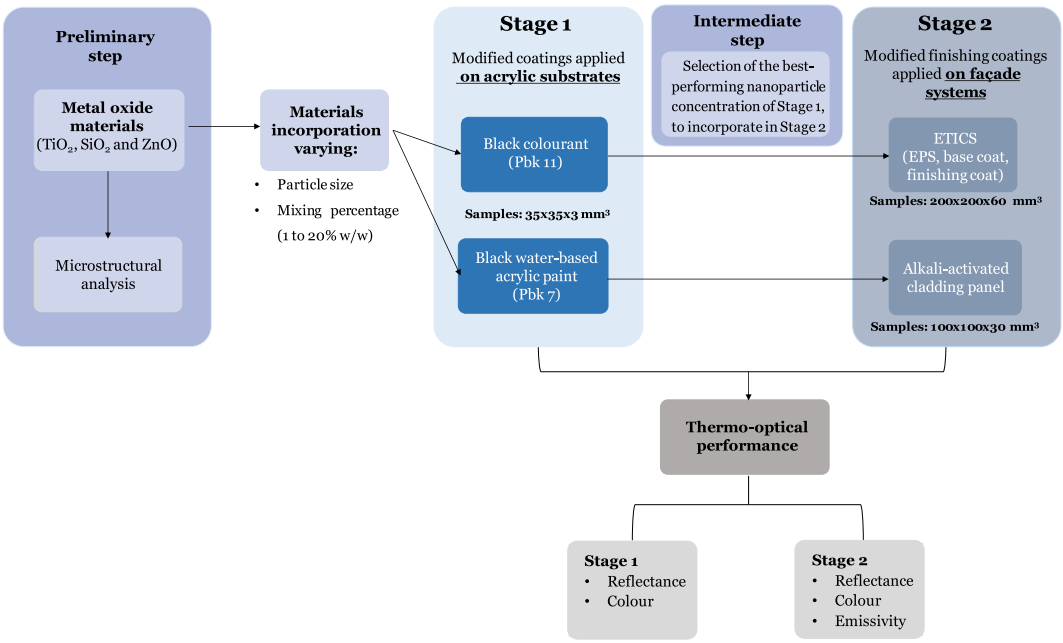


**Fig. 1.** Schematic representation of the experimental methodology.

**Table 1**
Nanoparticles' type, sizes and concentrations.

| Nanoparticle | Sizes (nm) | Concentration (% w/w) |
|---|---|---|
| Silicon dioxide ($SiO_2$) | 20-30, 60–70 and 400 | 1, 3, 5, 8, 12, 16 and 20 |
| Titanium dioxide ($TiO_2$) | 30 | |
| Zinc oxide (ZnO) | 10-30, 100, 500 and 1000 | |

**Table 2**
Colourant and paint characterisation.

| Name | Pigment | Colour | Index | Opacity | Density ($kg/m^3$) |
|---|---|---|---|---|---|
| Black colourant | $Fe_2O_4$ (magnetite) | Dark grey or black w/bluish to yellowish undertones | PBk11 | 2–3 | 1911 |
| Black water-based acrylic paint | Amorphous carbon black | Deep black, brown undertone | PBk7 | 1–2 | 1364 |

**Table 3**
Composition of the finishing coatings applied to the façade systems.

| Façade system | Sample | Dimensions of specimens (mm) | Nanoparticles | Size (nm) | % w/w nanoparticle | % w/w colourant |
|---|---|---|---|---|---|---|
| ETICS | Acrylic-based finishing coating | 200 × 200 × 60 | Without nanoparticles | | | |
| | Col1 | | $TiO_2$ | 30 | 8 % [a] | 6 % [b] |
| | Col2 | | ZnO | 500 | | |
| | Col3 | | $SiO_2$ | 60–70 | | |
| Cladding panel | Acrylic paint | 100 × 100 × 30 | Without nanoparticles | | | Non-applicable |
| | Coa1 | | $TiO_2$ | 30 | 8 % [c] | |
| | Coa2 | | ZnO | 500 | | |
| | Coa3 | | $SiO_2$ | 60–70 | | |

[a] Percentage relative to colourant weight.
[b] Percentage relative to the organic coating weight.
[c] Percentage/relative to acrylic-paint weight.

with sodium hydroxide (NaOH, 3 M) and sodium silicate (ratio of NaOH/silicate was 0.3). A 0.6 solid/liquid ratio was chosen to provide mechanical strength. After adding the activator, the specimens were cured in a controlled ambient (85 °C, 40 % HR) for about 20 h [36]. The finishing coating consists of black water-based acrylic paint.

The visual aspect of both types of samples is presented in Fig. 2.

### 2.2. Microstructural analysis of nanoparticles

The morphology and crystalline nature were assessed by Scanning Electron Microscopy (SEM) with analysis of Secondary Electron (SE) and Electron Backscattered Diffraction (EBSD) analysis (Quanta 400 FEG ESEM/EDX Genesis X4M) using an acceleration voltage of 15 kV. The SEM images were taken at × 20,000, × 50,000, × 100,000 and ×200000 magnifications.

### 2.3. Thermo-optical assessment of façade coatings

#### 2.3.1. Reflectance

Reflectance measurement can be carried out by measuring the solar spectrum properties such as absorbance, reflectance and transmittance of a material using a spectrophotometer. As such, a portable modular spectrophotometer was used coupled with different wavelengths (FLAME-T (UV-VIS) and FLAME-NIR) with an integrating sphere in the 200–1650 nm range (measured at 5 nm wavelength intervals along a spectrum, UV-VIS and NIR). The measuring is an adapted procedure of ASTM E903 [37], as described and

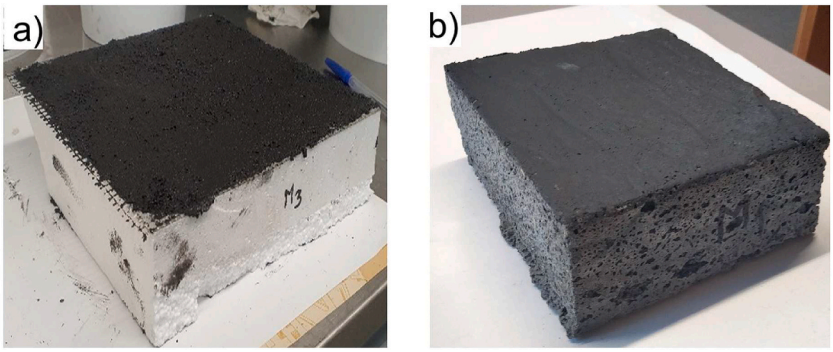


**Fig. 2.** Samples of (a) ETICS and (b) Alkali-activated cladding.

validated by Ramos et al. [38]. The total and the NIR reflectance were calculated using the select weighted ordinates in accordance with section 8.3.3 of ASTM E903 [37], considering a Direct Normal Irradiance for air mass of 1.5 defined in ASTM G197 [39]. Through the continuous reflectance measurement along the spectrum, it is possible to determine the total reflectance (SR) given by equation (1):

$$SR = \sum_{i=1}^{100} R(\lambda_i) \,/\, 100 \tag{1}$$

while the NIR Reflectance ($SR_{NIR}$) was calculated using equation (2):

$$SR_{NIR} = \sum_{i=46}^{100} R(\lambda_i) \,/\, 55 \tag{2}$$

where the subscript i is the ordinate number derived from the tables of ASTM G173 [40] in Appendix X2 of ASTM E903 [37], and R is the spectral reflectance given by the spectrophotometer at a given ordinate wavelength (λi). Three continuous measurements were carried out for each sample, and the average *SR* and $SR_{NIR}$ were presented.

### 2.3.2. Colourimetry parameters

The colourimetry parameters of all samples were studied using the same modular spectrophotometer, only in the UV-VIS region (400–700 nm). The CIE L*a*b colour coordinates were calculated as recommended by the Commission Internationale de l'Eclairage (CIE) [41] for the visible range, with the observer 10° under a D65 illuminant. According to the CIE methodology, the lightness (L*) ranges from black (zero) to white (100), the a* coordinate ranges from green (negative values) to red (positive values), and the b* of blue (negative) to yellow (positive).

The chroma ($C^*_{ab}$) is the colour intensity (i.e. light red, pastel red, dark red, etc.) perceptible to the human eye, whose value is defined in equation (3). The hue ($H_{ab}$) gives the colour type and identity for a dominant wavelength (red, blue, yellow, etc.) where the colour position is calculated by equation (4), corresponding in a circle position to red (0 or 360°), green (120°) and blue (240°). The average for the colour properties (L*, C*, H) was calculated considering three measurements for each sample.

$$C^*_{ab} = \left[(a^*)^2 + (b^*)^2\right]^{1/2} \tag{3}$$

$$H_{ab} = \text{arctang}(a^* \,/\, b^*) \tag{4}$$

The colour difference (ΔE) is a parameter expressing the perceived magnitude of the difference between two objects. The calculation of ΔE can be performed using equation (5) given on ISO 11664–4 [41]:

$$\Delta E^*_{ab} = \left[(\Delta L^*)^2 + (\Delta a^*)^2 + (\Delta b^*)^2\right]^{1/2} \tag{5}$$

Human eyes can perceive colour differences in different conditions (illuminant source, observed angle, and human psychological perceptibility). Several studies [42–44] defined a benchmark of the ΔE value between 2 and 3 for the human perceptible. This study considered the perception levels given in Table 4.

### 2.3.3. Emissivity

The emissivity of a material surface is its effectiveness in emitting energy as thermal radiation. The emissivity is the ratio between the thermal energy emitted by a real body and the thermal energy emitted by a blackbody at the same temperature. The emissivity measures were carried out using the standard procedures described in ASTM C1371 [46], which conceals a technique for determining the emissivity of typical material near room temperature using a portable differential emissometer. By measuring emissivity, it is possible to quantify the amount of long-wave electromagnetic radiation that a body emits and on which the surface temperature of the body depends. Thus, the values of emissivity can vary from 0 to 1.

## 3. Experimental results and discussion

### 3.1. Microstructural analysis of nanoparticles

A Scanning Electron Microscopy (SEM) exploration is displayed in Fig. 3. Such images show that 30 nm $TiO_2$ present a homogeneous and cubic shape [Fig. 3a]. As for the $SiO_2$ particles, it is observed that for the smaller sizes, i.e., 20–30 and 60–70 nm [Fig. 3 (b) and (c)], some agglomeration with spherical and homogenous morphology. However, for the 400 nm size, $SiO_2$ is observed in the irregular and large distribution of sizes [Fig. 3d]. The ZnO particles present polydispersity in terms of size and shape [Fig. 3e–(g)]. The

**Table 4**
Colour perception levels (after Xie et al. [45]).

| Level | ΔE | Perception |
|---|---|---|
| 0 | ≤1.0 | Not perceptible by human eyes |
| 1 | 1–2 | Perceptible by close observation |
| 2 | 2–10 | Perceptible with a glance |
| 3 | 11–49 | Colours are more similar than opposite |
| 4 | 100 | Colours are the exact opposite |

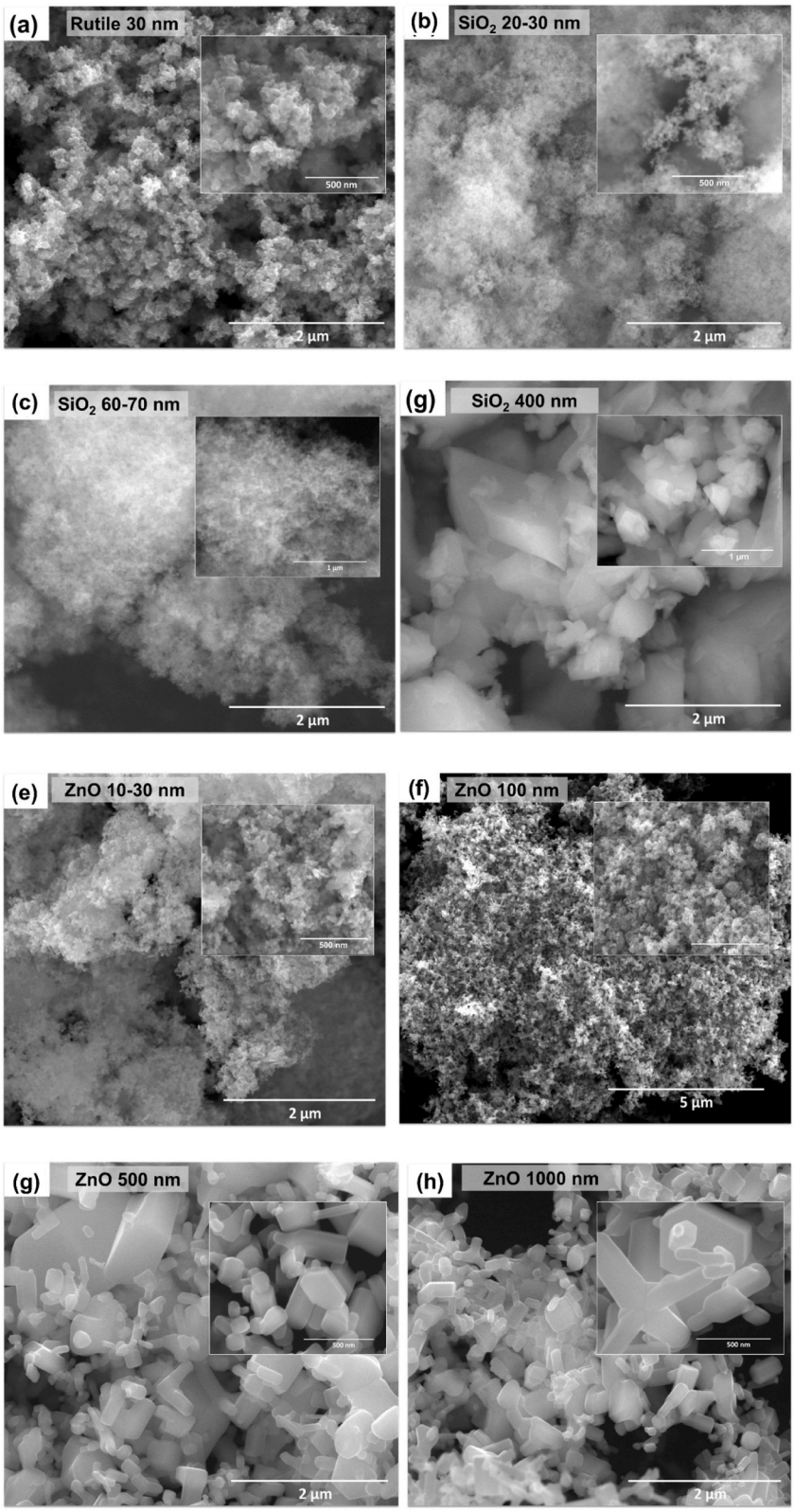


**Fig. 3.** SEM images of a low- and (inset) high-magnification of (a) the $TiO_2$ rutile 30 nm, (b) $SiO_2$ 20–30 nm, (c) $SiO_2$ 60–70, (d) $SiO_2$ 400 nm, (e) ZnO 10–30 nm, (f) ZnO <100 nm, (g) ZnO 500 nm and (h) ZnO 1000 nm.

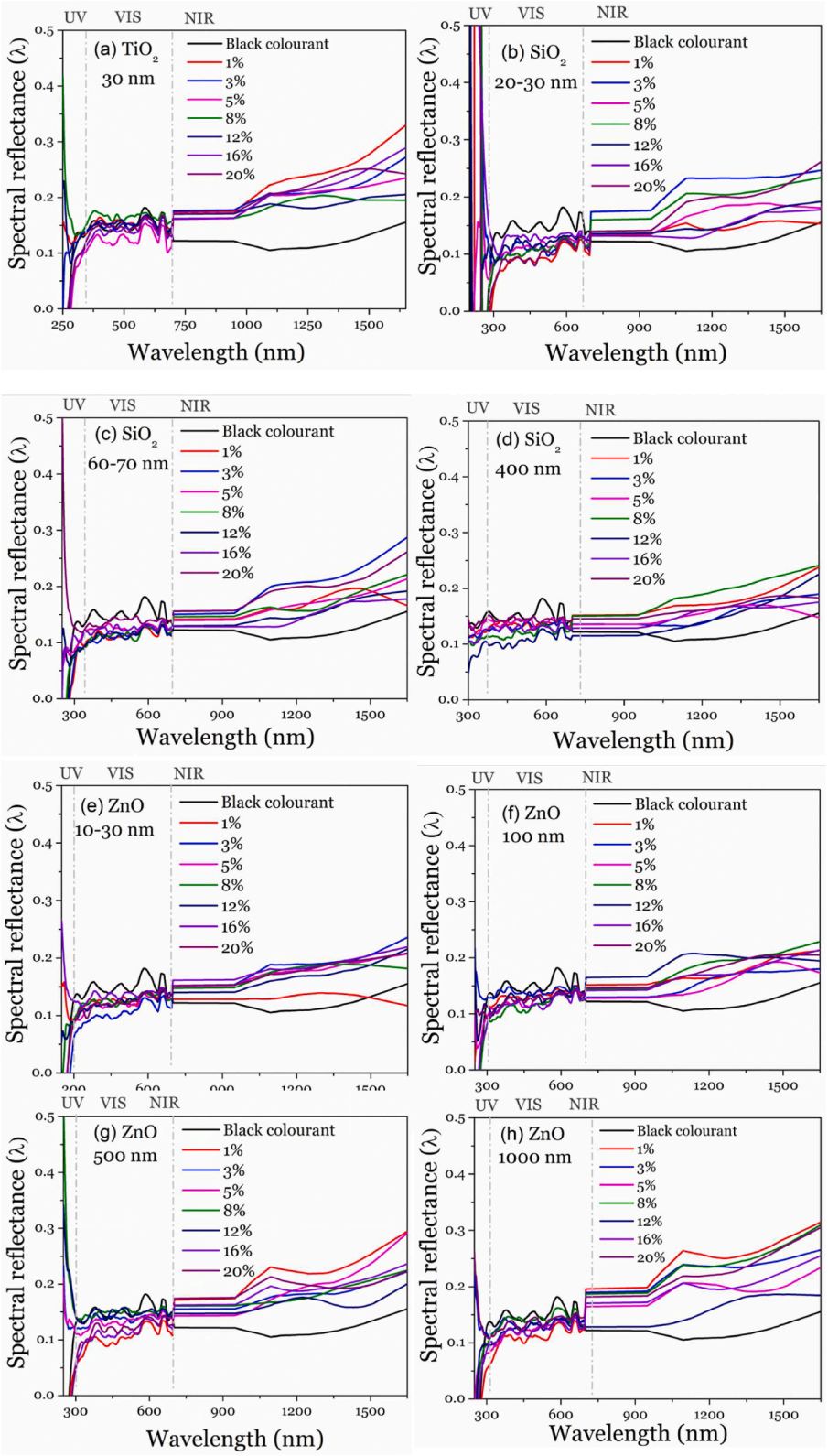


**Fig. 4.** Spectral reflectance behaviour for the black colourant modified with (a) the $TiO_2$ rutile 30 nm, (b) $SiO_2$ 20–30 nm, (c) $SiO_2$ 60–70 nm, (d) $SiO_2$ 400 nm, (e) ZnO 10–30 nm, (f) ZnO <100 nm, (g) ZnO 500 nm and (h) ZnO 1000 nm samples.

nanoparticles are spherical in Fig. 3e concerning the 10–30 nm size. For the <100 nm [Fig. 3f], the particle presents a shape of faceted crystals with homogeneous sizes. As for the 500 and 1000 nm [Fig. 3g and (h)], the particles are mixed in the form of nanorods and irregular size and shape.

### 3.2. Thermo-optical performance of the modified coatings

#### 3.2.1. Influence of nanoparticle type and concentration mixed in the colourant

The optical properties of the nanoparticle-mixed colourant samples were carried out to choose from each group of nanoparticles which size and percentage were suitable to incorporate in the ETICS finishing coating.

*3.2.1.1. Reflectance assessment.* Fig. 4 presents the spectral reflectance of the colourant-modified samples in acrylic substrates. Observing the results, it is possible to notice that all samples show an analogous performance in the UV-VIS region by partially absorbing the visible light. Concerning the near-infrared region, the specimens present significant differences since the nanoparticles-modified samples improve the reflectance of the colourant.

The results of the reflection in Fig. 5 show that an increase in the NIR reflection leads to an increase in the total reflectance in all cases and gives a correlation of 80 % for the studied samples. However, this behaviour of total reflectance versus NIR reflectance depends on the particle type, size, and incorporation ratio.

For $TiO_2$ (Fig. 5a), the total and NIR reflectance decrease with increasing particle incorporation. The best performance for these particles is obtained at 1 % incorporation, where the total reflectance increases by 20 % (up to 0.19) and the NIR reflectance by 95 % (up to 0.22).

When evaluating the $SiO_2$, Fig. 5b, it can be seen for all particle sizes that a shift in the behaviour of the two reflections occurs at 12 %. The best concentration is related to the particle size for this type of particle. Small particle size is expected to lead to a higher reflectance [47,48], but the best performance is obtained with a 20 % admixture of particles with a size of 60–70 nm, leading to an increase of 21 % (up to 0.17) overall and 52 % (up to 0.19) of the NIR reflectance.

The ZnO (Fig. 5c) shows the most inconsistent results when increasing the proportion of incorporated particles and decreasing the size. The best performance is seen with a ratio of 3 % of 1000 nm particle size, an overall increase of 35 % (up to 0.18) and an 87 % (up to 0.21) increase in NIR reflectance. This result has an opposite effect to that expected for size, as several studies indicate that reducing

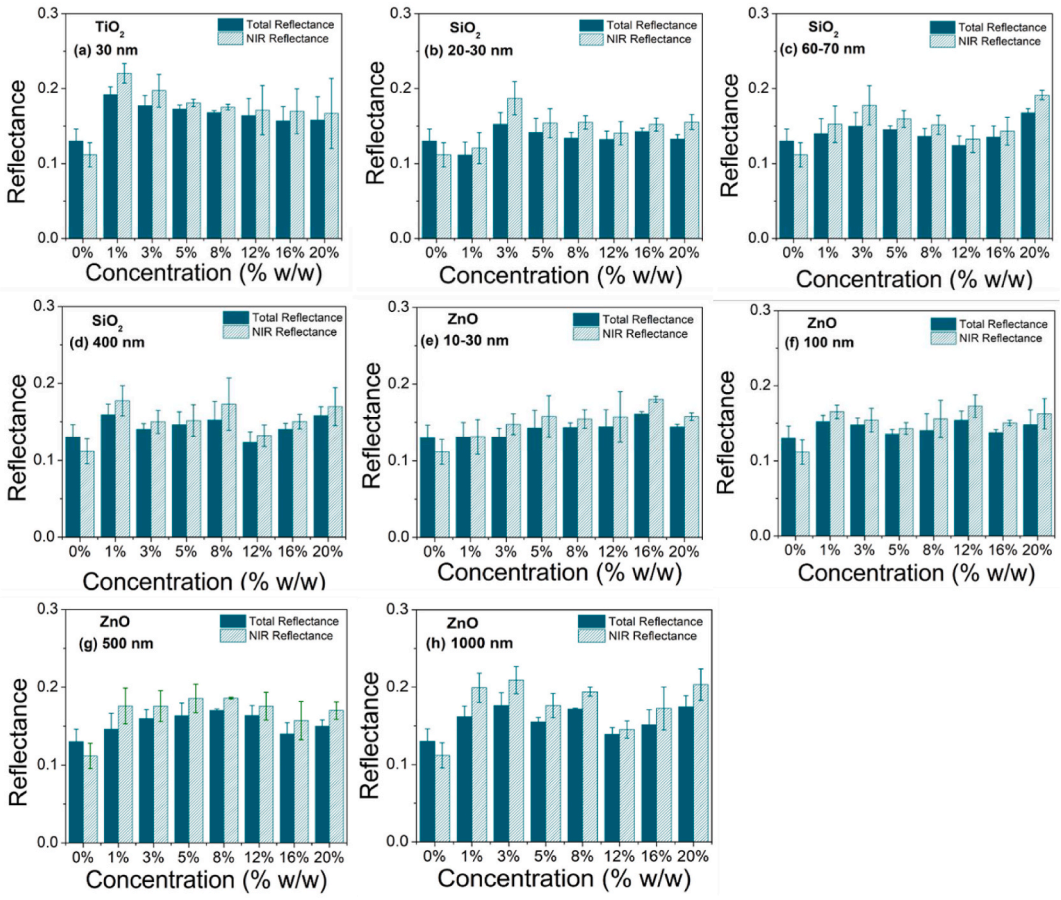


**Fig. 5.** Calculated total average and NIR reflectance for the black colourant mixed with (a) the $TiO_2$ rutile 30 nm, (b) $SiO_2$ 20–30 nm, (c) $SiO_2$ 60–70, (d) $SiO_2$ 400 nm, (e) ZnO 10–30 nm, (f) ZnO <100 nm, (g) ZnO 500 nm and (h) ZnO 1000 nm samples.

particle size can lead to a better reflection result [48,49]. Yet, the behaviour in the NIR region is similar to the results found by Ref. [50].

As expected, titanium oxide performs best in improving reflectance [47,51]. Nevertheless, the best combination of particle type, size, and content for application in architectural coatings also depends on the aesthetic evaluation.

*3.2.1.2. Colourimetric evaluation.* This study uses the CIELab colour space evaluation. Fig. 6 shows the a*b* coordinates for the colourant samples mixed with micro- and nanoparticles, while Fig. 7 shows the colour parameters hue and chroma assessment. The comparison of the visual aesthetics of the modified samples with the standard black colourant is shown in Fig. 8.

The a* and b* coordinates indicate the colour shades [52]. For the standard results, the values of these coordinates are related to the pigment used in the black dye (Table 2). The PBk11 has a bluish-to-yellowish hue [53], seen in Fig. 6a, with a b* value of almost zero and a positive value of a* and a hue value between 120° and 240° (Fig. 7a). The low value for chroma in Fig. 7a is also a characteristic of black colour. Similar results were obtained for all standard samples for $SiO_2$ (Figs. 6b and 7b) and ZnO (Figs. 6c and 7c). The black, white, and grey colours are considered achromatic, meaning that the difference between a* and b* should be minimal [52].

When evaluating the incorporation of the micro and nanoparticles, the best results are expected to be obtained for the samples with the smallest a*b* difference [54]. In the case of titanium oxide (Fig. 6a), the best incorporation rate would be 5 %. 16 % and 20 %, but when evaluating the chroma and hue difference (Fig. 7a), the 16 % leads to the lowest deviations. The best candidates for the $SiO_2$ (Fig. 6b) could be the samples mixed with 400 nm or 60–70 nm, with 20 % incorporation due to the lower difference from the standard in hue and chroma value (Fig. 7b). Similarly, when analysing reflectance, the results for the zinc oxide coordinates (Fig. 6c) are the most inconsistent, with the best achromatic values at the highest levels of incorporation, 16 % and 20 %. When looking for the minor differences in hue and chroma (Fig. 7c), the candidate for the best formulation is at 1000 nm with 20 %.

The hue and chroma values are based on the a* and b* coordinate measurements and form the basis of colour perception. Fig. 8a shows the colour difference and lightness for the modified samples compared to the black colourant without nanoparticles.

When analysing Fig. 8a for the samples mixed with $TiO_2$, it is noticeable that most of the samples have a colour difference of less than 2, corresponding to perception level 1, i.e. the difference is only noticeable when looking closely (description of the levels in Table 4). The inclusion in the 3 % content is the only one where the variation in lightness is negative, which was not expected as the negative values indicate that the sample is darker than the standard. This effect produces a higher colour difference than in the other samples (Fig. 8a). The best concentrations in terms of variation of brightness and colour are 8 % and 12 %.

As far as $SiO_2$ incorporation is concerned (Fig. 8b), the 60–70 nm and 400 nm sizes show the slightest colour variation (ΔE). For $SiO_2$, all samples became darker than the standard samples, which means negative values for ΔL in Fig. 8b, with the best doping combination found at the high incorporation levels, namely 16 % and 20 %, for all sizes.

The ZnO (Fig. 8c) sample shows the most significant variation in the change in results compared to the other particles. The best result for the ZnO particles is for the 1000 nm, where almost all samples show a colour difference of less than 2.

The results on colourant show that, as expected, the effect of the micro and nanoparticles on the thermo-optical properties of the dye depends on the type, size, and content of the incorporated nanoparticles [47]. For example, looking at the performance in

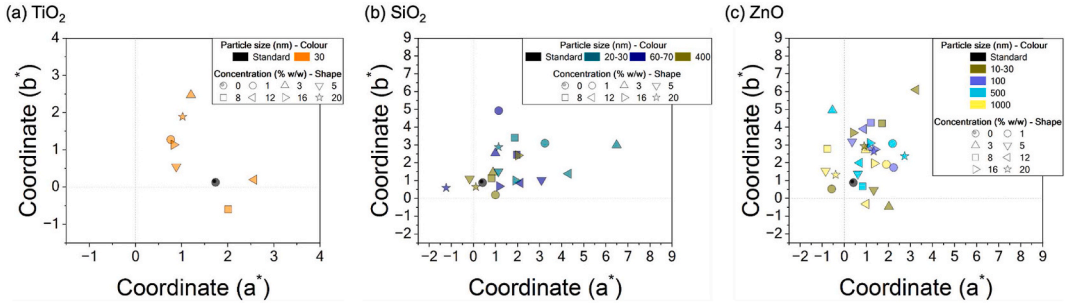


**Fig. 6.** CIELab space coordinates for black colourant mixed with (a) the $TiO_2$ rutile 30 nm, (b) $SiO_2$, and (c) ZnO particles.

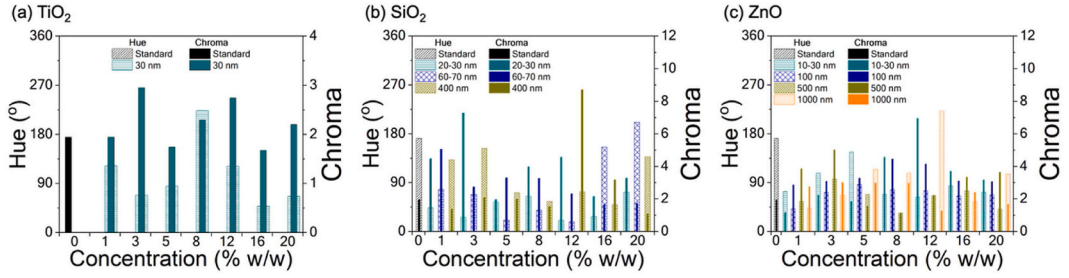


**Fig. 7.** Hue and chroma assessment for black colourant mixed with (a) the $TiO_2$ rutile 30 nm, (b) $SiO_2$ and (c) ZnO particles, when compared with the conventional colourant.

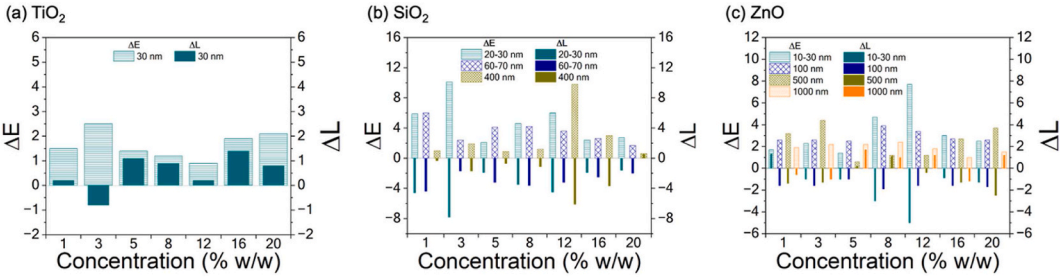


**Fig. 8.** Total colour difference and lightness variation for black colourant mixed with (a) the $TiO_2$ rutile 30 nm, (b) $SiO_2$ and (c) ZnO particles, when compared with the colourant without nanoparticles. (For interpretation of the references to colour in this figure legend, the reader is referred to the Web version of this article.)

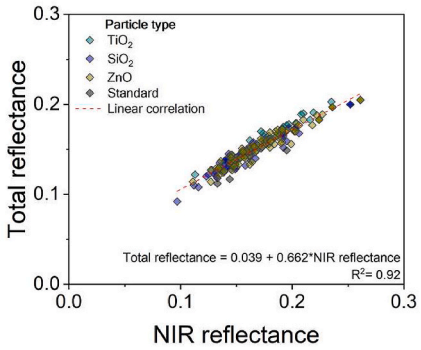


**Fig. 9.** Correlation between the NIR reflectance and Total reflectance.

reflection (total and NIR) and colour difference, it can be seen that the best particle is $TiO_2$. However, the zinc oxide could be more effective than the titanium oxide of level 1 in improving the NIR reflectance with level 2 colour differences. At the same time, the silica shows the worst performance in both criteria (colour and reflectance). Nevertheless, the total reflectance increased for all nanoparticles tested due to the effect of NIR reflectance, as shown in Fig. 9.

For the next phase, i.e. incorporation into the acrylic paint and the ETICS finishing coating, three particles with a size of 30 nm, 60–70 nm and 500 nm for $TiO_2$, $SiO_2$ and ZnO were selected for the paint and the ETICS, respectively. A concentration of 8 % was adopted for the final ETICS coating, as shown in the results of the decision matrix in Table 5.

The decision matrix used in Table 5 considers the study variables (particle type, size, and percentage) and their optical effects (colour and reflectance) on the coatings. Firstly, the variables with the most significant increase in NIR reflectance, followed by the lower value of ΔE, were selected. The second criteria were the highest total reflectance values and lower variation in the lightness.

In the case of ZnO, the 1000 nm size was not chosen due to the mixture agglomeration used in the façade systems. Also, 1000 nm and 500 nm particle sizes presented similar behaviour in total and the NIR reflectance.

### *3.2.2. Influence of nanoparticle type and concentration in acrylic paint*

Similar to the former study, the same procedure and measurements were carried out for the acrylic paint particle mixed in acrylic substrates to find the most suitable concentration of micro- and nanoparticles to be incorporated in the finishing coating of the alkali-activated cladding panel.

*3.2.2.1. Reflectance assessment.* Considering the previous results, the acrylic paint was mixed with $TiO_2$ 30 nm, $SiO_2$ 60–70 nm and ZnO 500 nm in size from 1 to 20 % concentration (w/w). Using this methodology, it is possible to compare total and NIR reflectance behaviour in two distinct coatings (colourant and acrylic paint) for the same substrate with the adequate size and percentage of the selected nanoparticles. Typical spectral reflectance variations are displayed in Fig. 10. Fig. 10a shows that $TiO_2$ nanoparticles increase the reflectance in both regions, particularly in the visible regions, which consequently will cause a colour change in the paint. The behaviour of the other two nanoparticle groups is similar since both absorb light in the visible region, although less than $TiO_2$. Analysing the $SiO_2$ nanoparticles, it is observed that there is an improvement in the near-infrared reflectance, specifically for concentrations between 1 % and 12 %. Likewise, ZnO microparticles cause an enhancement in the reflectance, but only at the lowest concentrations (1 % and 3 %), as verified in Fig. 10c.

The results of total and NIR reflectance, shown in Fig. 11, demonstrate that the incorporation of nanoparticles in the acrylic paint, in general, causes an increase in both values of reflectance. Acrylic paints have more components in their composition when compared to colourants, which have a simpler composition. This factor could influence the amount of radiation the particle-mixed samples reflect once a carbon-based pigment constitutes the acrylic paint. Through the sample production, it was verified that the incorporation of particles on the paint was simpler compared to the commercial colourant. In general, both averaged values of reflectance for each group tested are higher in acrylic paint when compared to the black colourant. ZnO microparticles are an exception. Even so, these

**Table 5**
Decision matrix for the best performance of thermo-optical properties for modified colourant samples.

| Variable | | | Modification against standard | | | |
|---|---|---|---|---|---|---|
| | | | Total reflectance | NIR reflectance | \|ΔL\| | ΔE |
| Particle | $TiO_2$ | | 31% | 41% | 0.8 | 1.7 |
| | $SiO_2$ | | 9% | 33% | 2.8 | 3.7 |
| | ZnO | | 16% | 50% | 1.5 | 2.7 |
| Particle size | $TiO_2$ | 30 | 31% | 41% | 0.8 | 1.7 |
| | $SiO_2$ | 20-30 | 4% | 17% | 3.7 | 4.8 |
| | | 60-70 | 10% | 42% | 2.7 | 3.5 |
| | | 400 | 12% | 41% | 2.0 | 2.8 |
| | ZnO | 10-30 | 10% | 38% | 1.9 | 3.3 |
| | | 100 | 12% | 41% | 1.6 | 2.9 |
| | | 500 | 20% | 57% | 1.2 | 2.4 |
| | | 1000 | 24% | 66% | 1.1 | 2 |
| C | 1% | | 15% | 45% | 1.8 | 3 |
| | 3% | | 19% | 50% | 2.1 | 3.6 |
| | 5% | | 16% | 41% | 1.4 | 1.9 |
| | 8% | | 17% | 45% | 2.0 | 2.9 |
| | 12% | | 10% | 32% | 2.8 | 4.3 |
| | 16% | | 12% | 37% | 1.8 | 2.7 |
| | 20% | | 19% | 49% | 1.2 | 2.2 |

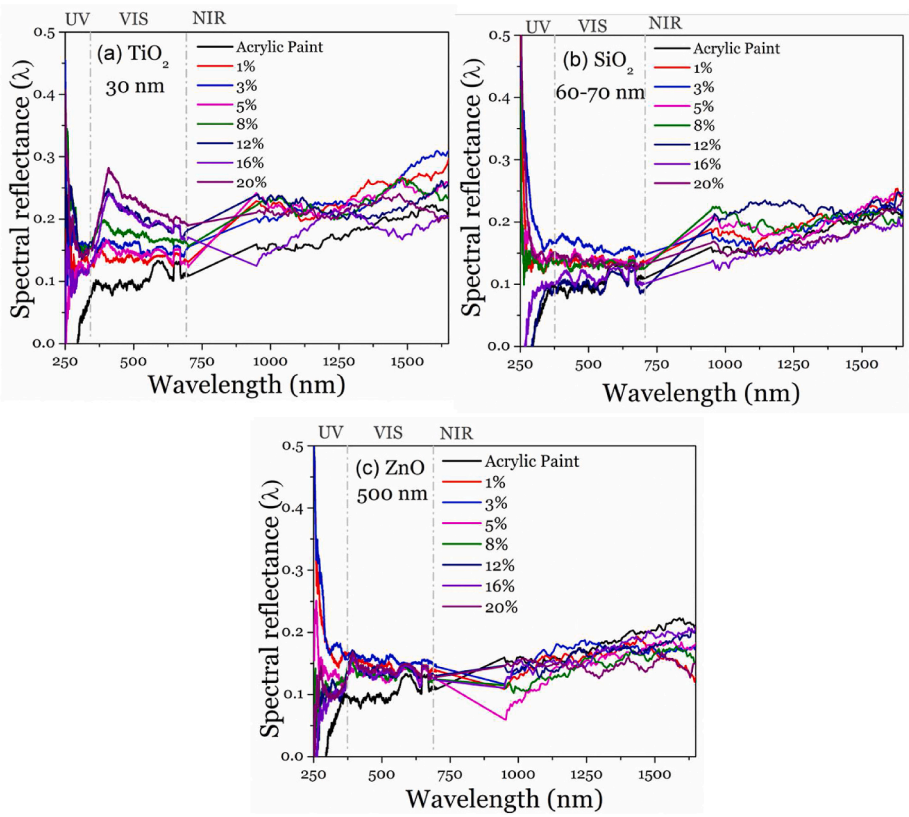


**Fig. 10.** Spectral reflectance behaviour for the acrylic paint mixed with (a) the $TiO_2$ rutile 30 nm, (b) $SiO_2$ 60–70 nm and (c) ZnO 500 nm samples.

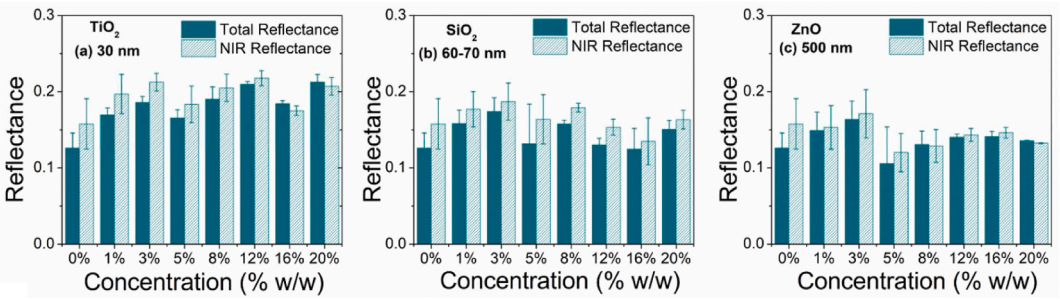


**Fig. 11.** Calculated total average and NIR for the acrylic paint mixed with (a) the $TiO_2$ rutile 30 nm, (b) $SiO_2$ 60–70 nm and (c) ZnO 500 nm samples.

samples show improved reflectance than the non-modified acrylic paint. Clearly, the $TiO_2$ nanoparticles show an improvement on both total and NIR results of 20 % and 22 %, respectively, for 20 % concentration, when compared to the 13 % of the non-modified paint, followed by the $SiO_2$ nanoparticles, which achieves the best result for 3 % concentration with 17 % of total reflectance. As for the ZnO, the modified samples present lower reflectance with 16 % of total reflectance for 3 % concentration.

*3.2.2.2. Colourimetric evaluation.* As described for the colourant, the effect of the micro- and nanoparticles in the acrylic paint depends on the colour pigment. In this study, the paint has a PBk7 pigment index classified as a deep black-brown undertone [53]. The brown is classified as an orange hue (+a* and +b* coordinates, Fig. 12a with low lightness [52]. As soon as the hue/chroma of the black acrylic paint deviates from the black colourant, the admixture of the particles shows a different behaviour, as can be seen from the hue and chroma values (Fig. 12b) and the total colour difference and lightness variation (Fig. 13).

Incorporating the micro and nanoparticles into the acrylic paint substantially influences the colour coordinates more than the black colourant. The acrylic paint has more components than the pigment, which could explain the variations in the incorporation of particles [42].

The deviations in the CIELab coordinates affect the hue and chroma of the samples (Fig. 12b). All samples with 16 % and 20 % $TiO_2$ have a negative effect on the hue, meaning that the colours take on a greyish tone and become brighter [52,55], which is confirmed by the variation in brightness in Fig. 13.

For the $TiO_2$, the 1 % and 3 % may be the best candidates as they show less variation in a* coordinate (Fig. 12a) and less total colour variation and lightness increase (Fig. 13). For the silicate, the higher concentrations, 8 %, 12 % and 16 %, show the best results and evaluate the hue and chroma (Fig. 12b). When considering the ΔL, the best concentration should be 16 % with a minimal change (Fig. 13). The ZnO shows the most achromatic CIELab values, with the lowest a*b* difference, but has the most significant impact on the hue (Fig. 12b). The best candidates are those with a content of 8 %, as they show less variation in total colour difference and brightness (Fig. 13).

None of the acrylic paint-modified samples has a total colour difference (ΔE) of less than 2. For $SiO_2$–3%, $TiO_2$ at 12 %/16 % and 20 %, the ΔE was above 10. The other samples have a colour perception at level 2, meaning the colour difference can be perceived at a glance.

Modifying the black acrylic paint also shows a good result in increasing the total reflectance by changing the NIR range. However, the effect on colour aesthetics was more pronounced than with the black colourant. Therefore, a new decision matrix, Table 6, was created to define the best concentration for applying the paint to the façade samples, considering the same criteria as Table 5.

Applying the criteria to increase NIR reflectance and total reflectance without changing colour aesthetics, the best-applied concentration in colour is 8 %, which increases NIR reflectance by 41 %, with a lower total colour difference (4.5).

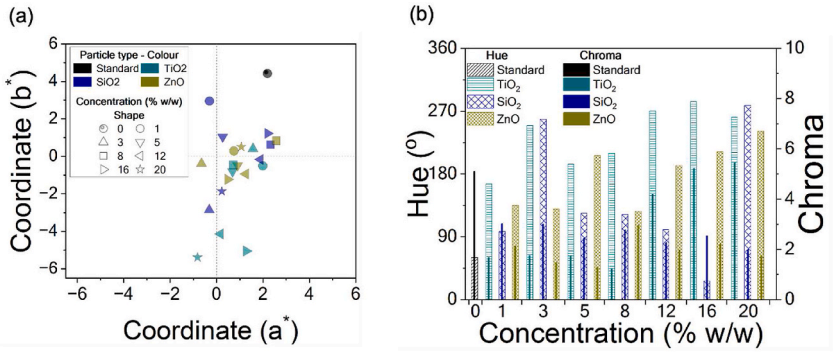


**Fig. 12.** CIELab space coordinate (a) and hue and chroma assessment (b) for the acrylic paint mixed with the selected particles.

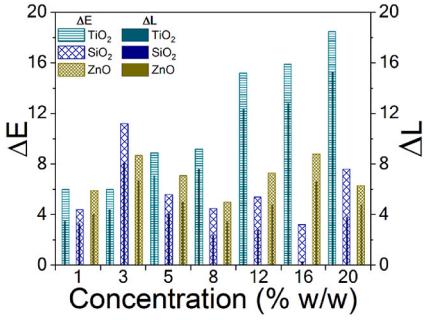


**Fig. 13.** Total colour difference and lightness variation of acrylic paint mixed with the selected particles. (For interpretation of the references to colour in this figure legend, the reader is referred to the Web version of this article.)

**Table 6**
Decision matrix for the best performance of thermo-optical properties for modified acrylic paint samples.

| Variable | | Modification against standard | | | |
|---|---|---|---|---|---|
| | | Reflectance | NIR reflectance | \|ΔL\| | ΔE |
| Particle | $TiO_2$ | 58% | 68% | 9.0 | 11.4 |
| | $SiO_2$ | 23% | 39% | 3.5 | 6.0 |
| | ZnO | 16% | 12% | 5.1 | 7.0 |
| Content | 1% | 34% | 45% | 3.6 | 5.5 |
| | 3% | 47% | 57% | 6.4 | 8.6 |
| | 5% | 13% | 29% | 5.4 | 7.2 |
| | 8% | 34% | 41% | 4.5 | 6.2 |
| | 12% | 34% | 41% | 6.7 | 9.3 |
| | 16% | 26% | 25% | 6.5 | 9.3 |
| | 20% | 40% | 38% | 8.0 | 10.8 |

### *3.3. Thermo-optical performance of façade systems with modified coatings*

#### *3.3.1. ETICS*

Fig. 14 shows the spectral and calculated reflectance for the ETICS samples, where the standard is considered to be the final coating mixed with the black colourant (6 % w/w), Col1 is considered to be the standard mixed with 8 % $TiO_2$ 30 nm, Col2 is considered to be 8 % ZnO 500 nm and Col3 is considered to be 8 % $SiO_2$ 60–70 nm.

The results of Cozza et al. [42] and Levinson et al. [56] indicate that dark colours have a reflectance in the visible range (VIS) of less than 20 %. As shown in Fig. 14a, all ETICS samples could be classified as a dark basis of the VIS reflectance, and a change in the UV and NIR range could also be detected in the modified samples (Col1, Col2 and Col3).

The NIR reflectance of the black standard ETICS sample (acrylic-based finishing coating) (Fig. 14b) is higher than the total reflectance value. This behaviour contrasts with the standard samples with a colourant (Total: 0.130 and NIR: 0.112, Fig. 5), where the

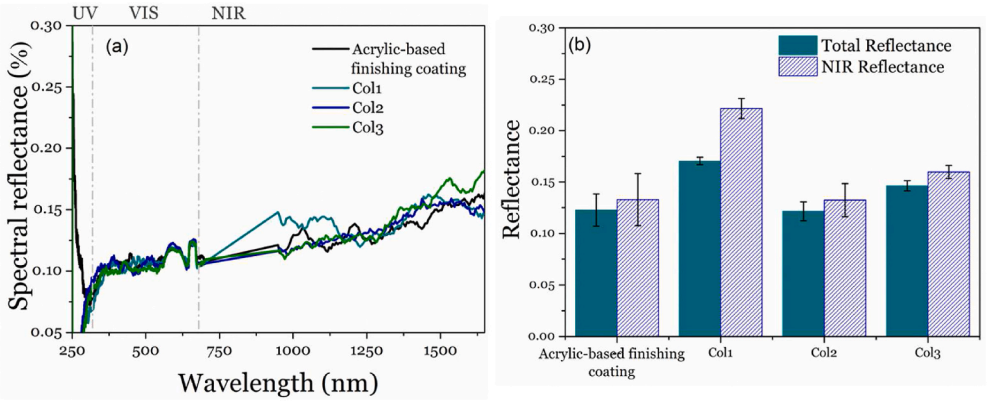


**Fig. 14.** (a) Spectral and (b) calculated total and NIR reflectance for the ETICS samples with particles' incorporation (Col1 – $TiO_2$; Col2 – ZnO; Col3 – $SiO_2$) and without (acrylic-based finishing coating).

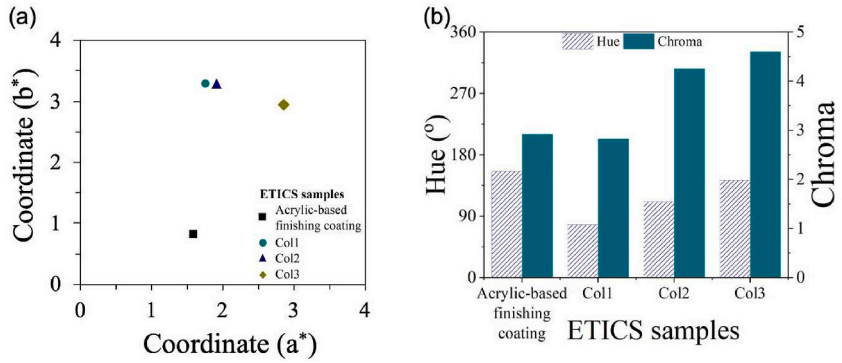


**Fig. 15.** Colour parameters of ETICS samples with and without the modified finishing coating: a) a* and b* CIELab coordinates b) Hue value. (For interpretation of the references to colour in this figure legend, the reader is referred to the Web version of this article.)

improvement in NIR reflectance due to the coating type was 98 % (colourant vs finishing coating). Similar results for the same colours on different coatings were observed by Alchapar and Correa [57].

Fig. 14b shows that $TiO_2$ (Col1) performs best in the NIR with an improvement of 65 % (0.22), followed by $SiO_2$ (Col3) with an improvement of 20 % (0.16) and ZnO (Col3), which does not change the reflectivity in the NIR. The best performance of the Col1 samples might be related to the high reflectance of the titanium oxide and the size of the nanoparticles [48,51]. The increase also affects the behaviour of the total reflectance in the NIR and agrees with the results of the samples mixed with a colourant (Table 5).

The aesthetic evaluation of the ETICS was based on the CIELab coordinates, Fig. 15a, and hue and chroma colour properties (Fig. 15b). The a*b* for the ETICS standard sample is similar to the colourant (Fig. 6) with a low a*b* value and a hue value between 120° and 240° but with a higher chroma value than the colourant (Fig. 7). If only CIELab coordinates are evaluated, titanium oxide (Col1) and silicon dioxide (Col3) are the best candidates for improving the thermo-optical properties.

The higher chroma values in Fig. 15b show that the ETICS samples are darker than the coloured ones [55], as Col1 maintains the chroma value compared to the standard and Col2 and Col3 increase the value by almost 50 %. This chroma improvement can also be

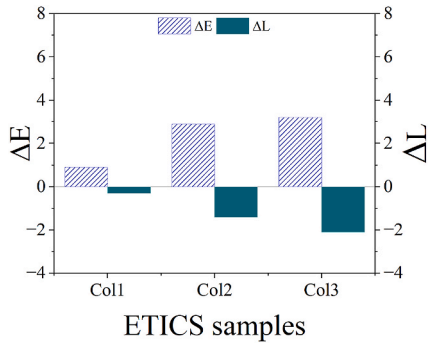


**Fig. 16.** Colour and lightness difference of ETICS samples with the modified finishing coating. (For interpretation of the references to colour in this figure legend, the reader is referred to the Web version of this article.)

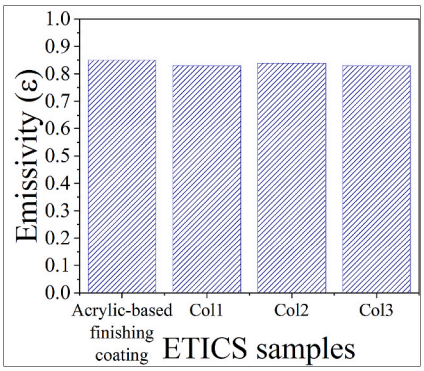


**Fig. 17.** Emissivity of ETICS samples coated with modified finishing coat.

seen in the brightness variation in Fig. 16.

The levels of colour perception for ETICS are level 1 for the Col1 samples and level 2 for the Col2 and Col3, as shown in Fig. 16. The modified sample became darker than the standard. Here, the best performance was demonstrated for the titanium oxide-mixed Col1 samples, an opposite effect than the 8 % $TiO_2$ inclusion in the colourant.

Another surface property essential to evaluate the temperature surface and the thermal behaviour of ETICS systems is the emittance, with results shown in Fig. 17.

The founded emissivity values, with an average value of 0.84, are consistent with the materials used for façade coatings [58]. The slight deviations in the results show that incorporating micro- and nanoparticles into the final coating of ETICS does not influence the emissivity, which is consistent with the results of Sharma et al. [59].

According to the criterion of improving the NIR reflectivity without changing the colour of commercial mortar for the final coating of ETICS, Col1 is the best formulation as it increases the NIR reflectivity by 65 % and has a colour difference of 0.9, while sample Col2 is the worst as it reduces the reflectivity by 1 % and results in a colour difference of 2.9.

### 3.3.2. *Cladding panel*

The thermo-optical properties, such as colour and reflection, are considered surface properties. Therefore, a cladding panel made of industrial/construction waste was painted with acrylic paint with and without incorporated particles (Table 3).

Fig. 18 shows the spectral and calculated reflectance for the cladding samples, considering the black acrylic paint as the standard, the 8 % $TiO_2$ 30 nm mixed as Coa1, 8 % ZnO 500 nm as Coa2 and 8 % $SiO_2$ 60–70 nm as Coa3.

As expected for dark colours in the visible range (VIS), 20 % should be lower [42,56]. Conversely, sample Coa1 (mixed with $TiO_2$) has a higher visible reflectance, Fig. 18a, while samples Coa2 and Coa3 can be classified as dark based on the VIS reflectance. The modified samples (Coa1, Coa2 and Coa3) also showed changes in the UV and NIR range.

The use of acrylic paint in the cladding panel (in Fig. 17b) shows the same behaviour as the acrylic paint in the acrylic substrate (Fig. 11). Meanwhile, all inclusions increase cladding reflectivity, unlike in ETICS. Coa2 (ZnO) presents as the best cladding formulation, increasing NIR reflectance by 27 %, while Coa3 causes an increase of 25 %, and Coa1 has the smallest gain of 2 %.

According to the criterion of colour aesthetics, the CIELab coordinates (Fig. 19a) of the standard samples have a similar value to the

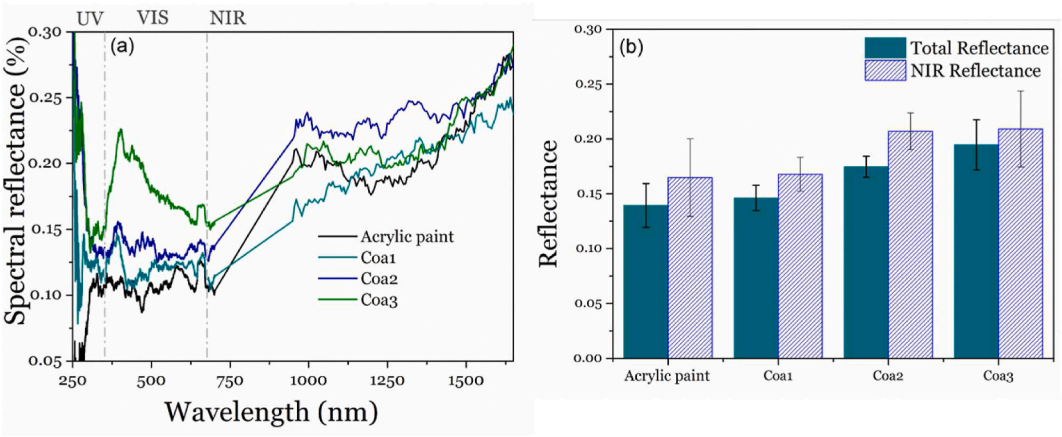


**Fig. 18.** (a) Spectral and (b) calculated total and NIR reflectance for the alkali-activated cladding samples with particles' incorporation (Coa1 – $TiO_2$; Coa2 – ZnO; Coa3 – $SiO_2$) and without (acrylic-based finishing coating).

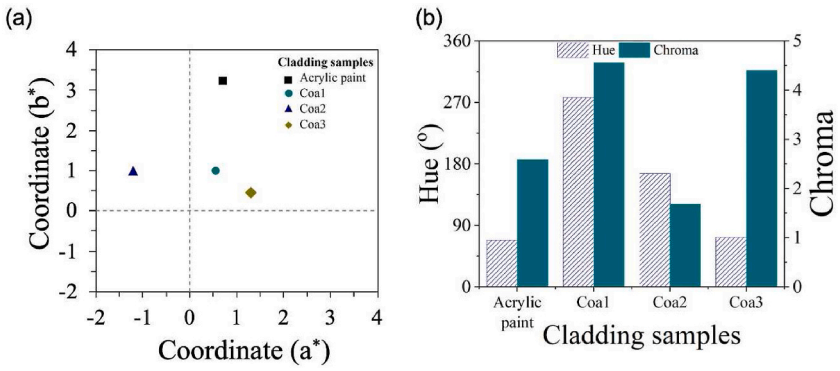


**Fig. 19.** Colour parameters of cladding samples with and without the modified acrylic paint: a) a* and b* CIELab coordinates b) Hue value. (For interpretation of the references to colour in this figure legend, the reader is referred to the Web version of this article.)

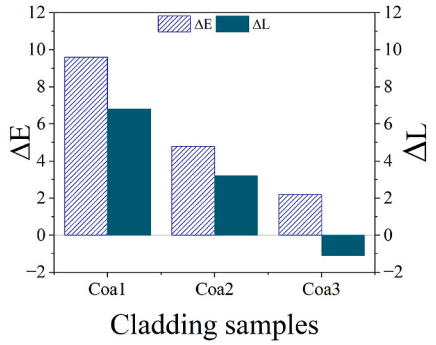


**Fig. 20.** Colour and lightness difference of cladding samples with the modified acrylic paint. (For interpretation of the references to colour in this figure legend, the reader is referred to the Web version of this article.)

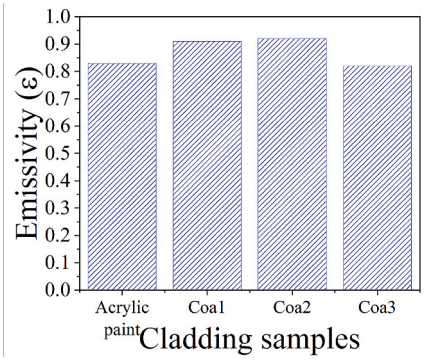


**Fig. 21.** Emissivity of cladding samples with the modified acrylic paint.

standard acrylic paint (Fig. 12a). In contrast, the admixture of nanoparticles, samples Coa1 and Coa2, decreases the coordinate values and changes the hue from orange to blue, as shown in Fig. 19b for the hue value above 90°.

On the criteria of colour aesthetic the CIELab coordinates (Fig. 19a), the standard samples have a similar value of the acrylic paint standard (Fig. 12a), while the incorporation of the nanoparticles, sample Coa1 and Coa2 reduce the coordinate values modifying the colour shade from orange to blue, as seen in Fig. 19b for the hue value higher than 90°. The best candidates under the colour parameters are Coa2 and Coa3 due to the lower hue and chroma variation.

Despite the colour parameters for aesthetic performance, evaluating the total colour difference (ΔE) and lightness (ΔL) is necessary (Fig. 20). In the case of the modified paint, the cladding becomes lighter with the incorporated nanoparticles, with the worse result for titanium oxide (Coa1) and the better for silica (Coa3). The levels of ΔE are higher than the ETICS rating, with the Coa1 and Coa2 formulations having level 2 and Coa3 having level 1 perception.

Emissivity is a thermal property that depends on surface characteristics, such as roughness and colour glow. In the case of the cladding samples (Fig. 21), no significant variation was found between the formulations, and an average value of 0.84, the same value as that of the ETICS and in the range of the façade materials.

According to the criterion of improving the NIR reflectance without changing the colour of the painted cladding, Coa1 is the best formulation as it increases the NIR reflectance by 25 % and has a colour difference of 2.2. In comparison, sample Coa2 increases the reflectance by 25 %, resulting in a colour difference of 4.8, and the worst formulation, Coa3, at a 2 % increase in the NIR range and a colour difference of 9.6.

## 4. Conclusions and perspectives

This work studied the effect of incorporating $TiO_2$, $SiO_2$ and ZnO micro- and nanoparticles on the thermo-optical properties of coatings for thermal enhanced façade systems, such as ETICS and waste-based cladding panels. It was found that.

- The thermo-optical performance depends on the type and size of the particles in a combination of the incorporated material;
- The reflectance measurements obtained through a spectrophotometer prove suitable for assessing the NIR reflectance of façade coatings. However, certain adjustments are required to align completely with the ASTM E903 standard;
- Comparing the same formulations for different applications, $TiO_2$ shows the best performance in ETICS, $SiO_2$ in acrylic paints and ZnO in colourant formulations;
- The titanium oxide is the best particle, improving NIR reflectance by 50 % with a ΔE of 3.4, while the zinc oxide improves NIR reflectance by 28 % with 3.2 from ΔE, and the $SiO_2$ improves NIR reflectance by 22 % with a total colour difference of 4.61;

- The colour aesthetics depend on the incorporated material, the lower ΔE for the colourant and the application of the pigment in the ETICS system; on average, the incorporation of the micro- and nanoparticles makes the colours lighter than the standard formulations in all cases studied.

These results show that it is possible to use different particles to meet the aesthetic requirements of using dark colours, to improve the thermo-optical behaviour and consequently to improve the durability of the different façade systems concerning thermal stress.

Building façades are susceptible to various wear and tear phenomena. Therefore, further evaluations of the durability of these modified top coatings for façade systems are needed and are also under development.

## CRediT authorship contribution statement

**Rita Carvalho Veloso:** Writing – original draft, Methodology, Investigation, Data curation, Conceptualization. **Joana Maia:** Writing – review & editing, Writing – original draft, Visualization, Supervision, Methodology, Investigation, Conceptualization. **Rodrigo Praça:** Visualization, Investigation. **Andrea Souza:** Writing – original draft, Formal analysis, Data curation, Conceptualization. **Andrea Souza:** Writing – original draft, Formal analysis, Conceptualization. **João Ventura:** Resources, Funding acquisition. **Nuno M.M. Ramos:** Writing – review & editing, Resources, Project administration, Funding acquisition. **Helena Corvacho:** Writing – review & editing, Writing– Original draft preparation, Supervision, Methodology, Conceptualization.

## Declaration of competing interest

The authors declare that they have no known competing financial interests or personal relationships that could have appeared to influence the work reported in this paper.

## Data availability

Data will be made available on request.

## Acknowledgements

This work was financially supported by Project PTDC/ECI-CON/28766/2017—POCI-01–0145-FEDER-028766 funded by FEDER through COMPETE2020—Programa Operacional Competitividade e Internacionalização (POCI) and by national funds (PIDDAC) through FCT/MCTES, Project Circular2B - 37_CALL#2 - Circular Construction in Energy-Efficient Modular Buildings financing under the Environment, Climate Change and Low Carbon Economy Programme within the scope of the European Economic Area Financial Mechanism EEA Grants 2014–2021 and by Base Funding - UIDB/04708/2020 with DOI 10.54499/UIDB/04708/2020 (https://doi.org/10.54499/UIDB/04708/2020) and Programmatic Funding - UIDP/04708/2020 with DOI 10.54499/UIDP/04708/2020 (https://doi.org/10.54499/UIDP/04708/2020) of the CONSTRUCT - Instituto de I&D em Estruturas e Construções - funded by national funds through the FCT/MCTES (PIDDAC). R. C. Veloso and A.R. Souza would like to acknowledge the support of FCT - Fundação para a Ciência e a Tecnologia for the funding of the Doctoral Grant SFRH/BD/148785/2019 and DFA/BD/8418/2020, respectively.

## References

[1] EC, In Focus: Energy Efficiency in Buildings, 2020. https://commission.europa.eu/news/focus-energy-efficiency-buildings-2020-02-17_en. (Accessed 18 July 2023).
[2] A. Brambilla, G. Salvalai, M. Imperadori, M.M. Sesana, Nearly zero energy building renovation: from energy efficiency to environmental efficiency, a pilot case study, Energy Build. 166 (2018) 271–283.
[3] M. Santamouris, Heat island research in europe: the state of the art, Adv. Build. Energy Res. 1 (1) (2007) 123–150.
[4] S. Wenninger, C. Kaymakci, C. Wiethe, Explainable long-term building energy consumption prediction using QLattice, Appl. Energy 308 (2022) 118300.
[5] M. Jowkar, A. Temeljotov-Salaj, C.M. Lindkvist, M. Støre-Valen, Sustainable building renovation in residential buildings: barriers and potential motivations in Norwegian culture, Construct. Manag. Econ. 40 (3) (2022) 161–172.
[6] S. Capelo, T. Soares, I. Azevedo, W. Fonseca, M.A. Matos, Design of an energy policy for the decarbonisation of residential and service buildings in northern Portugal, Energies 16 (5) (2023) 2239.
[7] L. Chen, G. Msigwa, M. Yang, A.I. Osman, S. Fawzy, D.W. Rooney, P.-S. Yap, Strategies to achieve a carbon neutral society: a review, Environ. Chem. Lett. 20 (4) (2022) 2277–2310.
[8] Y.H. Chan, Y. Zhang, T. Tennakoon, S.C. Fu, K.C. Chan, C.Y. Tso, K.M. Yu, M.P. Wan, B.L. Huang, S. Yao, H.H. Qiu, C.Y.H. Chao, Potential passive cooling methods based on radiation controls in buildings, Energy Convers. Manag. 272 (2022) 116342.
[9] A.L. Pisello, E. Fortunati, C. Fabiani, S. Mattioli, F. Dominici, L. Torre, L.F. Cabeza, F. Cotana, PCM for improving polyurethane-based cool roof membranes durability, Sol. Energy Mater. Sol. Cell. 160 (2017) 34–42.
[10] G.M. Revel, M. Martarelli, M.A. Bengochea, A. Gozalbo, M.J. Orts, A. Gaki, M. Gregou, M. Taxiarchou, A. Bianchin, M. Emiliani, Nanobased coatings with improved NIR reflecting properties for building envelope materials: development and natural aging effect measurement, Cement Concr. Compos. 36 (2013) 128–135.
[11] K. Dornelles, R. Caram, E. Sichieri, Natural weathering of cool coatings and its effect on solar reflectance of roof surfaces, Energy Proc. 78 (2015) 1587–1592.
[12] M. Santamouris, A. Synnefa, T. Karlessi, Using advanced cool materials in the urban built environment to mitigate heat islands and improve thermal comfort conditions, Sol. Energy 85 (12) (2011) 3085–3102.
[13] A. Cánovas-Saura, A. Cabrera-Lozoya, J. Padilla, Aesthetic Possibilities of Building Thermal Control through Colored Envelopes 13 (3) (2023) 802.
[14] N.M.M. Ramos, J. Maia, A.R. Souza, R.M.S.F. Almeida, L. Silva, Impact of incorporating nir reflective pigments in finishing coatings of ETICS, Infrastructure 6 (6) (2021), 79-79.
[15] M. Baneshi, S. Maruyama, H. Nakai, A. Komiya, A new approach to optimizing pigmented coatings considering both thermal and aesthetic effects, J. Quant. Spectrosc. Radiat. Transfer 110 (3) (2009) 192–204.
[16] W.E. Vargas, A. Amador, G.A. Niklasson, Diffuse reflectance of TiO2 pigmented paints: spectral dependence of the average pathlength parameter and the forward scattering ratio, Opt Commun. 261 (1) (2006) 71–78.

[17] M.-D. Cheng, W. Miller, J. New, P. Berdahl, Understanding the long-term effects of environmental exposure on roof reflectance in California, Construct. Build. Mater. 26 (1) (2012) 516–526.
[18] Y. Wu, P. Krishnan, M.-H. Zhang, L.E. Yu, Using photocatalytic coating to maintain solar reflectance and lower cooling energy consumption of buildings, Energy Build. 164 (2018) 176–186.
[19] M. Sleiman, T.W. Kirchstetter, P. Berdahl, H.E. Gilbert, S. Quelen, L. Marlot, C.V. Preble, S. Chen, A. Montalbano, O. Rosseler, H. Akbari, R. Levinson, H. Destaillats, Soiling of building envelope surfaces and its effect on solar reflectance – Part II: development of an accelerated aging method for roofing materials, Sol. Energy Mater. Sol. Cell. 122 (2014) 271–281.
[20] J. Maia, M. Pedroso, N.M.M. Ramos, P.F. Pereira, I. Flores-Colen, M.G. Gomes, L. Silva, Hygrothermal performance of a new thermal aerogel-based render under distinct climatic conditions, Energy Build. 243 (2021) 111001.
[21] J. Maia, N.M.M. Ramos, R. Veiga, Evaluation of the hygrothermal properties of thermal rendering systems, Build. Environ. 144 (2018) 437–449.
[22] M. Suwan, N. Sangwong, S. Supothina, Effect of Co and Pr doping on the properties of solar-reflective ZnFe2O4 dark pigment, IOP Conf. Ser. Mater. Sci. Eng. 182 (1) (2017) 012003.
[23] Q. Wang, F. Lai, W. Shi, X. Li, R. Chen, H. Liu, X. Zhang, Q. Chang, Y. Wang, Synthesis and color properties of MnTiO3 black ceramic pigment, Mater. Chem. Phys. 296 (2023) 127310.
[24] E.S.S. Cozza, M. Alloisio, A. Comite, G. Di Tanna, S. Vicini, NIR-reflecting properties of new paints for energy-efficient buildings, Sol. Energy 116 (2015) 108–116.
[25] R.C. Veloso, A. Souza, J. Maia, N.M.M. Ramos, J. Ventura, Nanomaterials with high solar reflectance as an emerging path towards energy-efficient envelope systems: a review, J. Mater. Sci. 56 (36) (2021) 19791–19839.
[26] C. Dias, R.C. Veloso, J. Maia, N.M.M. Ramos, J. Ventura, Oversight of radiative properties of coatings pigmented with TiO2 nanoparticles, Energy Build. 271 (2022).
[27] F.N. Jones, M.E. Nichols, S.P. Pappas, Pigments, Organic Coatings: Science and Technology, John Wiley & Sons, Inc., 2007, pp. 417–434.
[28] S. Bashir, J. Liu, Chapter 1 - nanomaterials and their application, in: J.L. Liu, S. Bashir (Eds.), Advanced Nanomaterials and Their Applications in Renewable Energy, Elsevier, Amsterdam, 2015, pp. 1–50.
[29] F. Wegner, Bounds on the density of states in disordered systems, Z. Phys. B Condens. Matter 44 (1) (1981) 9–15.
[30] D. Papadaki, G. Kiriakidis, T. Tsoutsos, Chapter 11 - applications of nanotechnology in construction industry, in: A. Barhoum, A.S. Hamdy Makhlouf (Eds.), Fundamentals of Nanoparticles, Elsevier, 2018, pp. 343–370.
[31] I. Alfieri, A. Lorenzi, L. Ranzenigo, L. Lazzarini, G. Predieri, P.P. Lottici, Synthesis and characterization of photocatalytic hydrophobic hybrid TiO2-SiO2 coatings for building applications, Build. Environ. 111 (2017) 72–79.
[32] M. Torabi-Kaveh, M. Moshrefyfar, S. Shirzaei, S.M.A. Moosavizadeh, B. Ménendez, S. Maleki, Application of resin-TiO2 nanoparticle hybrid coatings on travertine stones to investigate their durability under artificial aging tests, Construct. Build. Mater. 322 (2022).
[33] J.D. Bersch, I. Flores-Colen, A.B. Masuero, D.C.C. Dal Molin, Photocatalytic TiO2-based coatings for mortars on facades: a review of efficiency, Durability, Sustain. 13 (1) (2023) 186.
[34] Z. Lu, Q. Ge, Y. Zhang, G. Lian, Preparation and analysis of multi-scale colored superhydrophobic coatings with excellent mechanical strength and self-cleaning properties, J. Build. Eng. 64 (2023).
[35] EOTA, EAD 040083-00-0404, External Thermal Insulation Composite Systems (ETICS) with Rendering, European Organisation for Technical Approvals, Brussels, 2019.
[36] N. Cristelo, J. Maia, N.M.M. Ramos, J. Rivera, J. Ventura, R.C. Veloso, A. Fernández-Jiménez, Development of highly porous alkaline cements from industrial waste for thermal insulation of building envelops, Construct. Build. Mater. 409 (2023) 134068.
[37] ASTM, ASTM E903: Standard Test Method for Solar Absorptance, Reflectance, and Transmittance of Materials Using Integrating Sphere, ASTM International, West Conshohocken, PA, USA, 2020.
[38] N.M.M. Ramos, A.R. Souza, J. Maia, R.M.S.F. Almeida, Solar reflectance of ETICS finishing coatings - a comparison of experimental techniques, E3S Web of Conf. 172 (2020), 21003-21003.
[39] ASTM, ASTM G173: Standard Tables for Reference Solar Spectral Irradiances: Direct Normal and Hemispherical on 37° Tilted Surface, ASTM International, West Conshohocken, PA, USA, 2020.
[40] ASTM, ASTM G197-14: Standard Table for Reference Solar Spectral Distributions: Direct and Diffuse on 20° Tilted and Vertical Surfaces, ASTM International, West Conshohocken, PA, USA, 2021.
[41] ISO, Colorimetry - Part 4: CIE 1976 L*a*b* Colour Space, European Committe for Standardization, Brussels, 2007.
[42] E.S. Cozza, M. Alloisio, A. Comite, G. Di Tanna, S. Vicini, NIR-reflecting properties of new paints for energy-efficient buildings, Sol. Energy 116 (2015) 108–116.
[43] W.S. Mokrzycki, M. Tatol, Colour difference ΔE - a survey, MG& V 20 (4) (2011) 383–411.
[44] J.L. Parracha, G. Borsoi, R. Veiga, I. Flores-Colen, L. Nunes, A.R. Garcia, L.M. Ilharco, A. Dionisio, P. Faria, Effects of hygrothermal, UV and SO2 accelerated ageing on the durability of ETICS in urban environments, Build. Environ. 204 (2021) 108151.
[45] N. Xie, H. Li, H.J. Zhang, X. Zhang, M. Jia, Effects of accelerated weathering on the optical characteristics of reflective coatings for cool pavement, Sol. Energy Mater. Sol. Cell. 215 (2020).
[46] ASTM, ASTM C1371- Standard Test Method for Determination of Emittance of Materials Near Room Temperature Using Portable Emissometers, ASTM International, West Conshohocken, PA, USA, 2022.
[47] S. Kinoshita, A. Yoshida, Investigating performance prediction and optimization of spectral solar reflectance of cool painted layers, Energy Build. 114 (2016) 214–220.
[48] N. Xie, H. Li, A. Abdelhady, J. Harvey, Laboratorial investigation on optical and thermal properties of cool pavement nano-coatings for urban heat island mitigation, Build. Environ. 147 (October 2018) (2019) 231–240.
[49] M. Baneshi, S. Maruyama, H. Nakai, A. Komiya, A new approach to optimizing pigmented coatings considering both thermal and aesthetic effects, J. Quant. Spectrosc. Radiat. Transf. 110 (3) (2009) 192–204.
[50] M. Baneshi, S. Maruyama, A. Komiya, Comparison between aesthetic and thermal performances of copper oxide and titanium dioxide nano-particulate coatings, J. Quant. Spectrosc. Radiat. Transf. 112 (7) (2011) 1197–1204.
[51] M. Ullah, H.J. Kim, J.G. Heo, D.K. Roh, D.S.D.S. Kim, Sodium titanate as an infrared reflective material for cool roof application, J. Ceram. Process. Res. 20 (Special Issue 1) (2019) 86–91.
[52] A.K.R. Choudhury, Colour and Appearance Attributes, 2014, pp. 103–143.
[53] D. Myers, The Color of Art Pigment Database: Pigment Black, PBk, 2013. https://www.artiscreation.com/black.html#ci_pigment_black. Aug 2023.
[54] K.L. Uemoto, N.M.N.N. Sato, V.M. John, Estimating thermal performance of cool colored paints, Energy Build. 42 (1) (2010) 17–22.
[55] A.R.R. Hanson, What Is Colour? Elsevier, United Kingdom, 2012, pp. 3–21.
[56] R. Levinson, P. Berdahl, H. Akbari, Solar spectral optical properties of pigments - Part II: survey of common colorants, Sol. Energy Mater. Sol. Cell. 89 (4) (2005) 351–389.
[57] N.L.L. Alchapar, E.N.N. Correa, Comparison of the performance of different facade materials for reducing building cooling needs, in: F. Pacheco-Torgal, J. Labrincha, L. Cabeza, A. Granqvist (Eds.), Eco-Efficient Materials for Mitigating Building Cooling Needs, Woodhead Publishing, 2015, pp. 155–194.
[58] F. Ascione, L. Bellia, P. Mazzei, F. Minichiello, Solar gain and building envelope: the surface factor, Build. Res. Inf. 38 (2) (2010) 187–205.
[59] R. Sharma, S. Tiwari, S.K. Tiwari, Highly reflective nanostructured titania shell: a sustainable pigment for cool coatings, ACS Sustain. Chem. Eng. 6 (2) (2018) 2004–2010.